Figure S1. Overall distribution of whisk cycle phases of touch events for all units with rapid response to touch. Plot of the relative frequency of touch events at different phases of the whisk cycle. The blue horizontal line indicates the mean probability of touch over all phase intervals. The shaded region around this line indicates 95 % confidence limits for a uniform distribution. Although touch events near retraction are significantly less frequent, a sufficient number of these events occur in each session to produce stable touch response estimates, e.g., the mean number of touch events per session for the interval at the start of protraction (the lowest bar on the plot) is 12 touches per session. In general, each interval had at least 8 touches per individual session in the data sets that we analyzed.

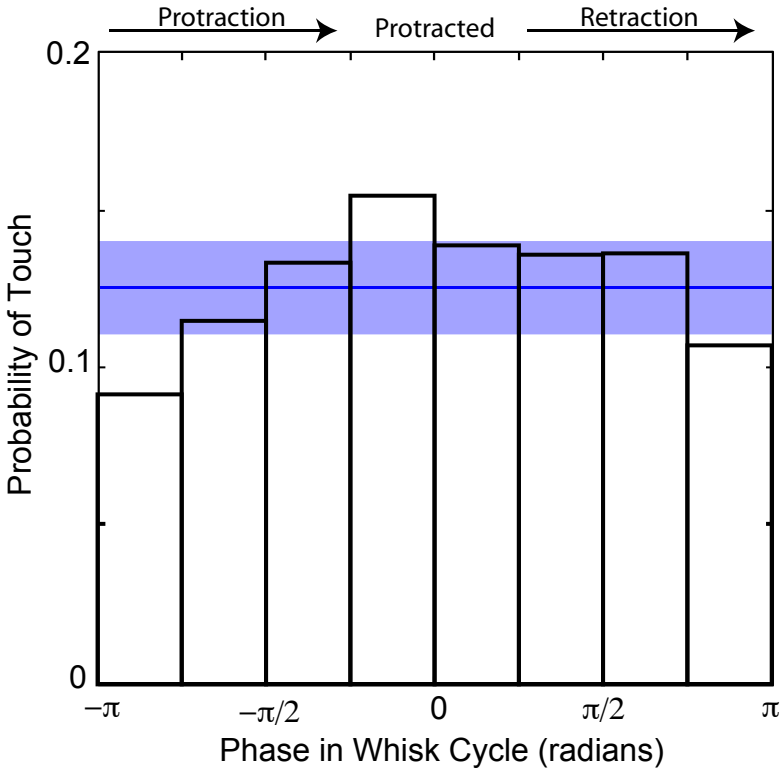

Nature Neuroscience: doi:10.1038/nn.2283

Figure S1 - Curtis and Kleinfeld

Figure S2. Example of raw data for a unit with a touch response modulated by whisking. Plots of high speed video frames, videographic position signal, rectified touch sensor signal, rectified (and low pass filtered) EMG signal, and S1 cortex recording channels surrounding two touch events during a recording session. Dots indicate times of contact events and sorted spike times for two units (waveforms and autocorrelations are shown at the bottom). The left plots show the rat touching the sensor during retraction and touch in the right plots is during protraction. Unit 1 is rapidly excited by touch and Unit 2 does not respond to touch. The spike activity of Unit 1 is modulated by free whisking and its touch response is modulated by whisking. The preferred phases of free whisking and touch for Unit 1 are near retraction, i.e., $\phi_{whsik} = 0.84\,\pi$ for whisking and $\phi_{touch} = 0.82\,\pi$ for touch. The touch event to the left is within the preferred phase of Unit 1 as can be seen by increased spiking briefly after touch is initiated. The touch event to the right occurs nearly opposite to the preferred phase of Unit 1 and spiking briefly after touch remains similar to background activity.

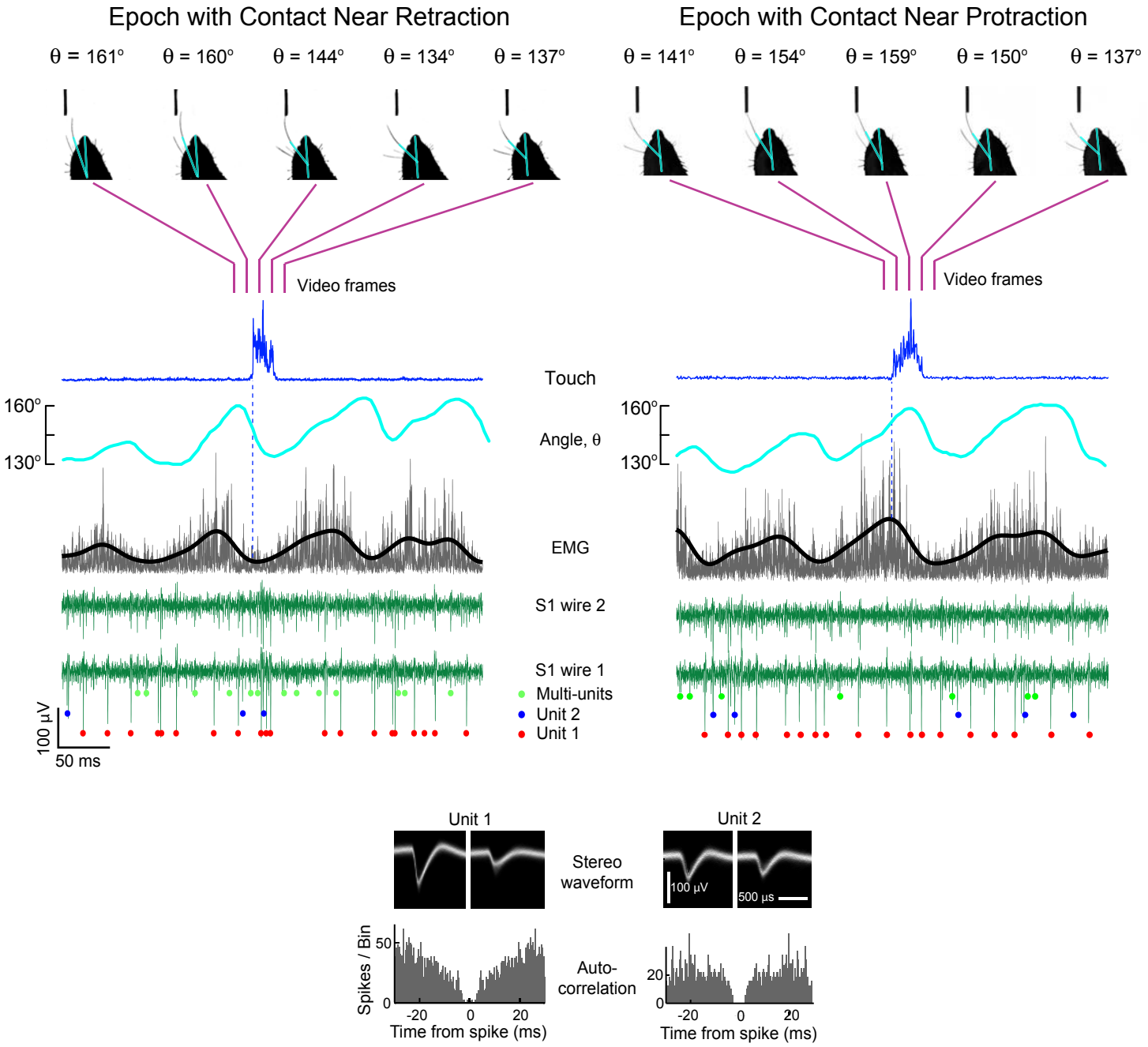

Nature Neuroscience: doi:10.1038/nn.2283

Figure S2 - Curtis and Kleinfeld

Figure S3. Distribution of touch response widths. Histogram of the width of the response to touch (full width at half maximum amplitude) for all excited or inhibited touch responses, *i.e.*, rapid excited, slow excited, and slow inhibited. Units with no response to touch are not included. Note that all rapid excited touch response widths fall within the first bin of the plot.

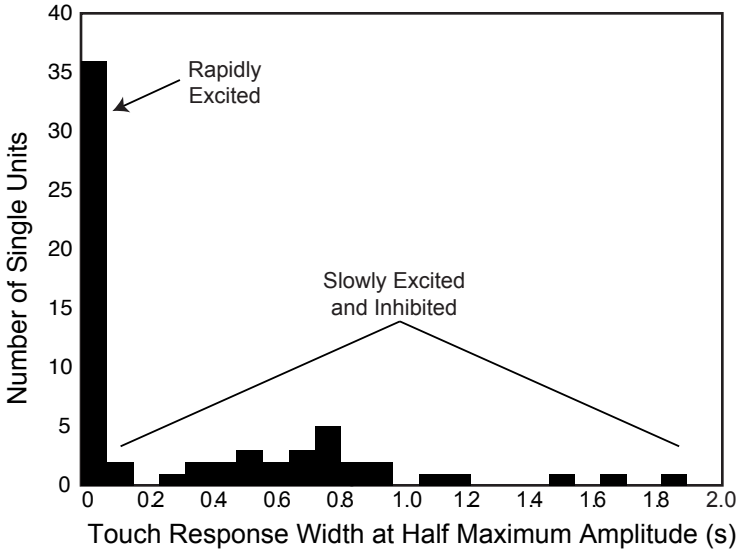

Nature Neuroscience: doi:10.1038/nn.2283

Figure S3 - Curtis and Kleinfeld

Figure S4. Free whisking modulation depths and spike waveform widths for all units according to touch response type. **(Top)** The distribution of different classes of single units according to the width, measured from peak to trough, of the waveform for the unit. The inserts show typical waveforms. **(Lower)** Free whisking modulation depth, measured from minimum to maximum divided by mean spike rates, plotted as functions of spike waveform width for the three difference responses, i.e., rapid excited, slow excited, and slow inhibited, as well as unresponsive cells.

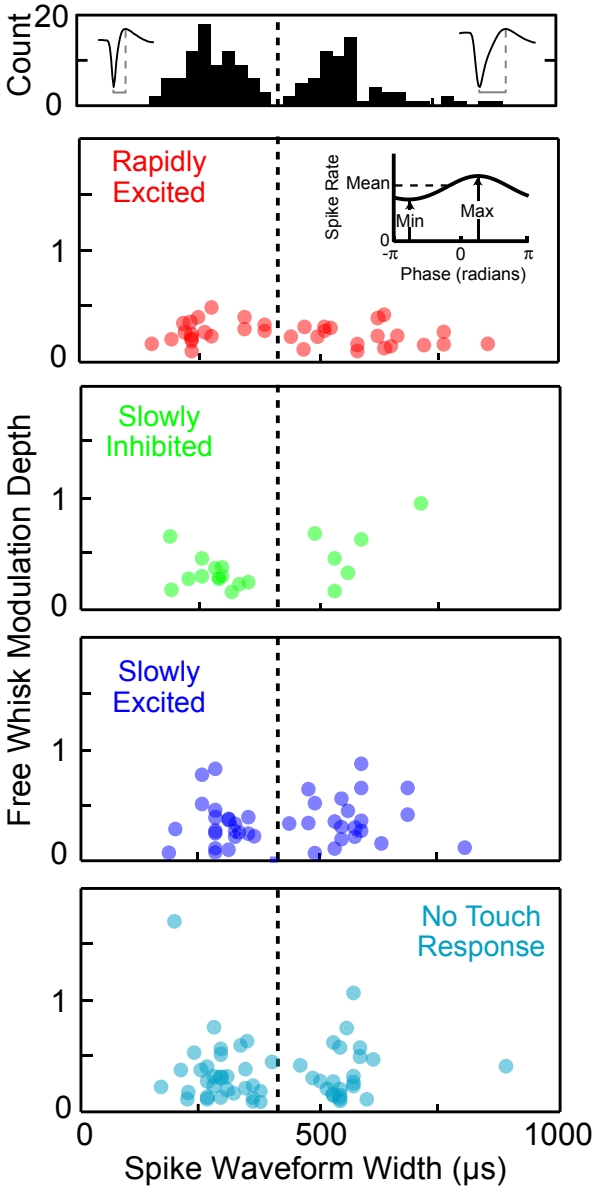

Nature Neuroscience: doi:10.1038/nn.2283

Figure S4 - Curtis and Kleinfeld

Figure S5. Probability of burst generation by single units in S1 vibrissa cortex. To quantify bursting activity in neurons excited by touch as opposed to free whisking in air, we produced separate interspike interval (ISI) histograms (bin width < 0.5 ms) for spikes that occurred during touch versus free whisking trials. To model normal spike activity, we used a generic form of the Inverse Gaussian equation to capture the refractory period spiking and exponential decay in number of ISI's at higher values. Bursting activity was modeled as a Gaussian function where the center and width were chosen manually such that the function was confined to the relative refractory period. If a particular ISI histogram contained a distinct peak at small values, which is indicative of bursting, the center and width of the Gaussian function were adjusted to best fit the peak. Functions were fit to the ISI histograms using Poisson distributed maximum likelihood estimates. Since particular ISI distributions were modeled as a linear combination of the Gaussian and Inverse Gaussian functions, the number of ISI values contributed by each could be calculated separately. Thus the number of ISI values that resulted from bursting was calculated by taking the difference in number of ISI values between the Gaussian and Inverse Gaussian fitted curves (bursting and normal spiking) and the Inverse Gaussian fitted curve (normal spiking only). The number of ISI values due to bursting was then divided by the total number of ISI values in order to compare the relative amount of bursting among different ISI distributions, i.e., between free whisking and touch trials of the same neuron as well as among different neurons.

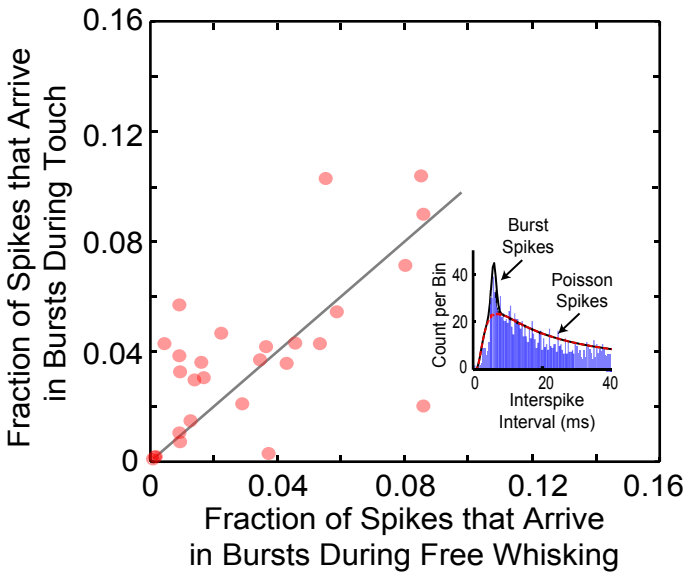

Nature Neuroscience: doi:10.1038/nn.2283

Figure S5 - Curtis and Kleinfeld

Figure S6. Laminar distribution and spike widths of different classes of single units. **(A)** Representative local field potential (LFP) measurements along with the current source density (CSD) calculated from these measurements. The CSD, shown also in false color to emphasize sinks and sources of current, was used to classify the cortical layer and depth for each recording. The plot on the right confirms that at least the short-time measurements concur with the past results of Swadlow, Gusev and Bezdudnaya (Activation of a cortical column by a thalamocortical impulse. 2002. J Neurosci 22, 7766-7779). **(B)** Compendium of responses across all single-units. **(C)** The laminar distribution of single-units that responded to active touch, independent of their whisking related response.

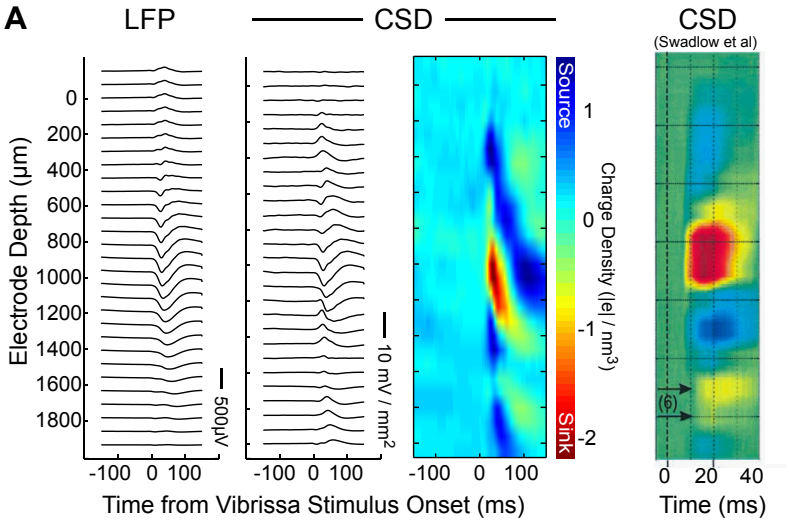

B

Touch Response	Whisking Response: Yes	Whisking Response: No
Rapidly Excited	20 %	3 %
Slowly Inhibited	9 %	4 %
Slowly Excited	15 %	13 %
None	19 %	17 %
	63 %	37 %

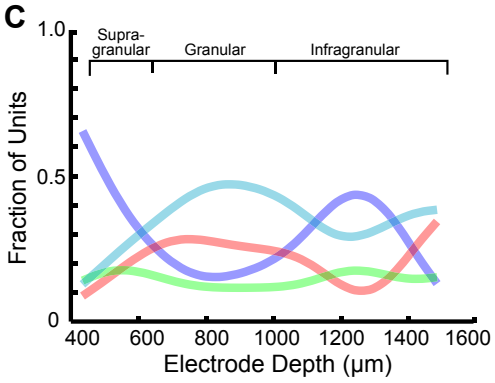

Nature Neuroscience: doi:10.1038/nn.2283

Figure S6 - Curtis and Kleinfeld

Figure S7. Examples of whisking activity that surrounds touch events. Each plot shows whisking activity that surrounds touch events that are sorted by where touch occurs in the whisk cycle. The data applies to the three units included in figure 4. Single whisking trajectories are thin lines overlaid in grey and mean trajectories are thick black lines. The lower plots show the relative frequencies of touch at different whisk cycle phases for each unit's recording session.

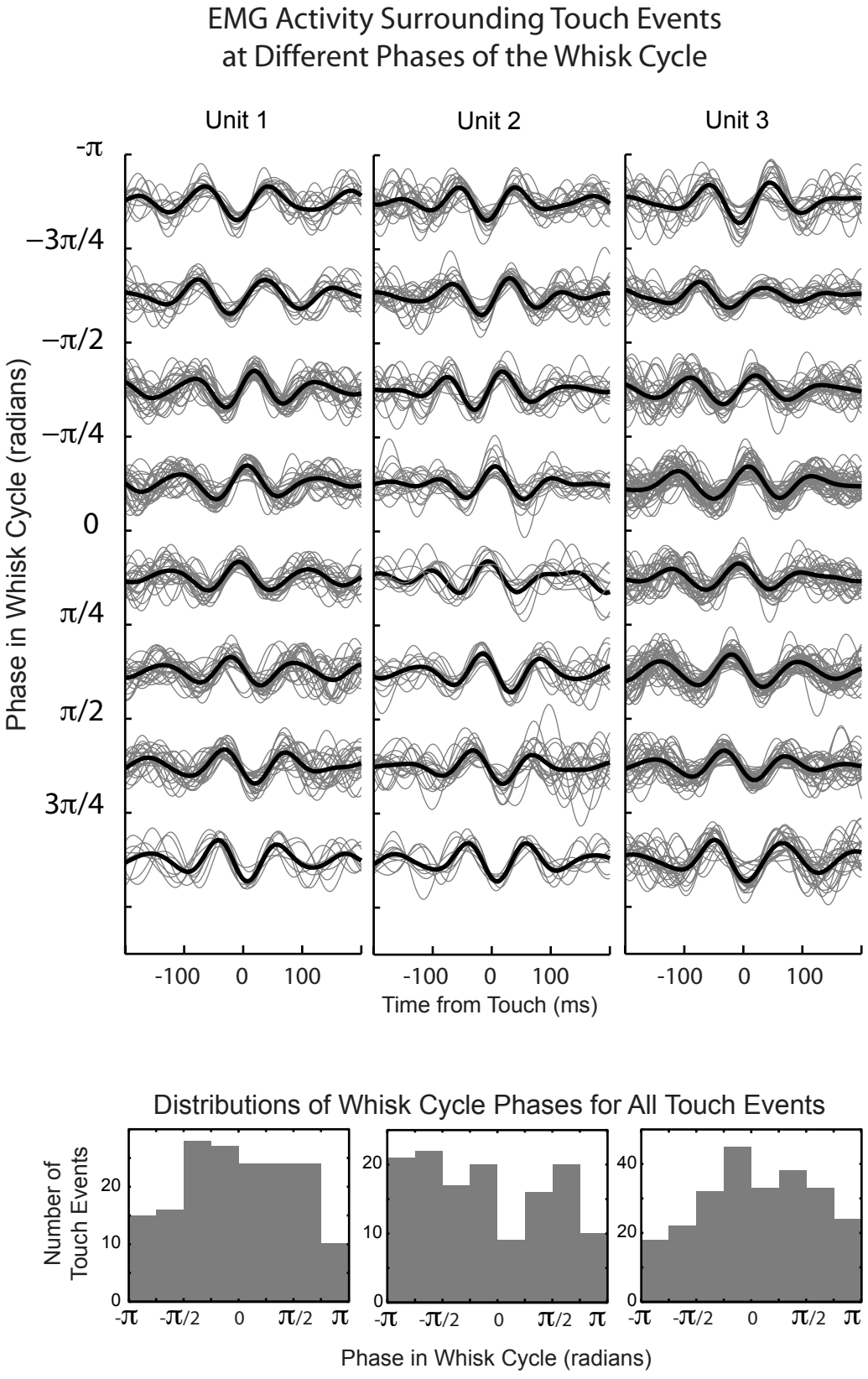

Nature Neuroscience: doi:10.1038/nn.2283

Figure S7 - Curtis and Kleinfeld

Figure S8. Free whisking and touch responses for all units with rapid response to touch that are significantly modulated by phase in the whisk cycle. Autocorrelations and waveforms for each neuron are plotted at the right end of each row. **(A1–A4).** Average spike response histograms in response to free whisking centered on ∇EMG peaks with sinusoid fits (green lines) and resultant parameters, i.e., DC = average spike rate across histograms, Amp = amplitude of sinusoid fit (DC to peak), ϕ = preferred phase, mod = response modulation depth. **(B1–B4)** Average spike responses to touch with BARS fits (green lines). Peak and baseline rates calculated from smooth curve are listed above each plot. **(C1–C4)** Left: Average touch response histograms parsed by phase in the whisk cycle using ∇EMG data to determine the phase. Right: Plots of the peak values of the touch response from fits to each of the eight intervals of the smooth curve touch responses in the left hand panels. The parameters listed above each plot were estimated by fitting a sinusoid to each curve and have the same designation as in panel A. Dotted lines indicate 95 % confidence intervals for mean spike rate estimates. **(D1–D4)** Left: Average touch response histograms parsed by phase in the whisk cycle using videographic data to determine the phase. Right: Plots of the peak values of the touch response from fits to each of the eight intervals of the smooth curve touch responses in the left hand panels. **(E1–E4)** Left: Average touch response histograms parsed by speed in the whisk cycle using videographic data to determine the speed. Right: Plots of the peak values of the touch response from GLM fits to each of the eight intervals of the smoothed touch responses in the left hand panels. **(F1–F4)** Left: Average touch response histograms parsed by angular position in the whisk cycle using videographic data to determine the position. Right: Plots of the peak values of the touch response from GLM fits to each of the eight intervals of the smoothed touch responses in the left hand panels.

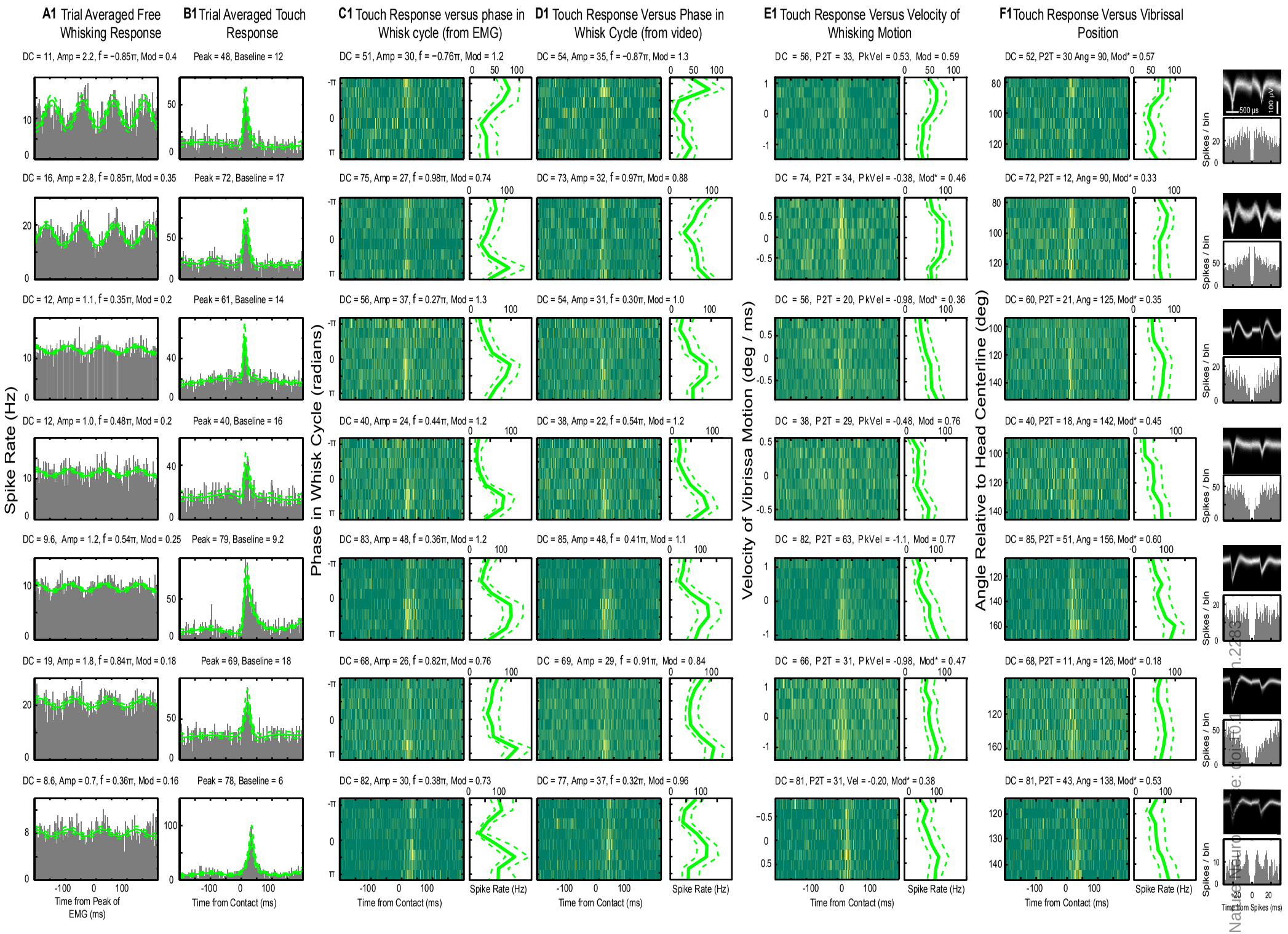

Figure S8 (1-7) - Curtis and Kleinfeld

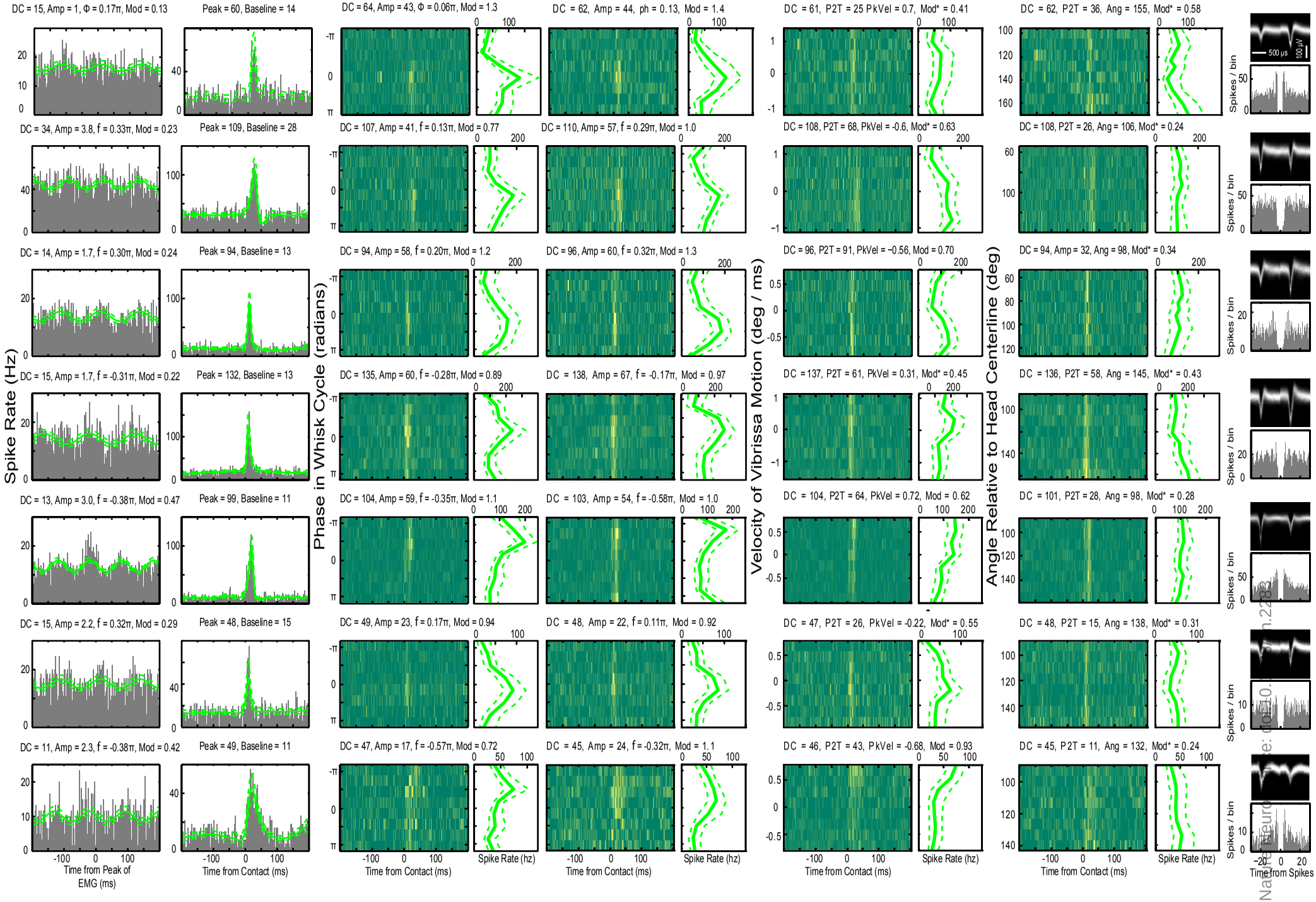

Figure S8 (8-14) - Curtis and Kleinfeld

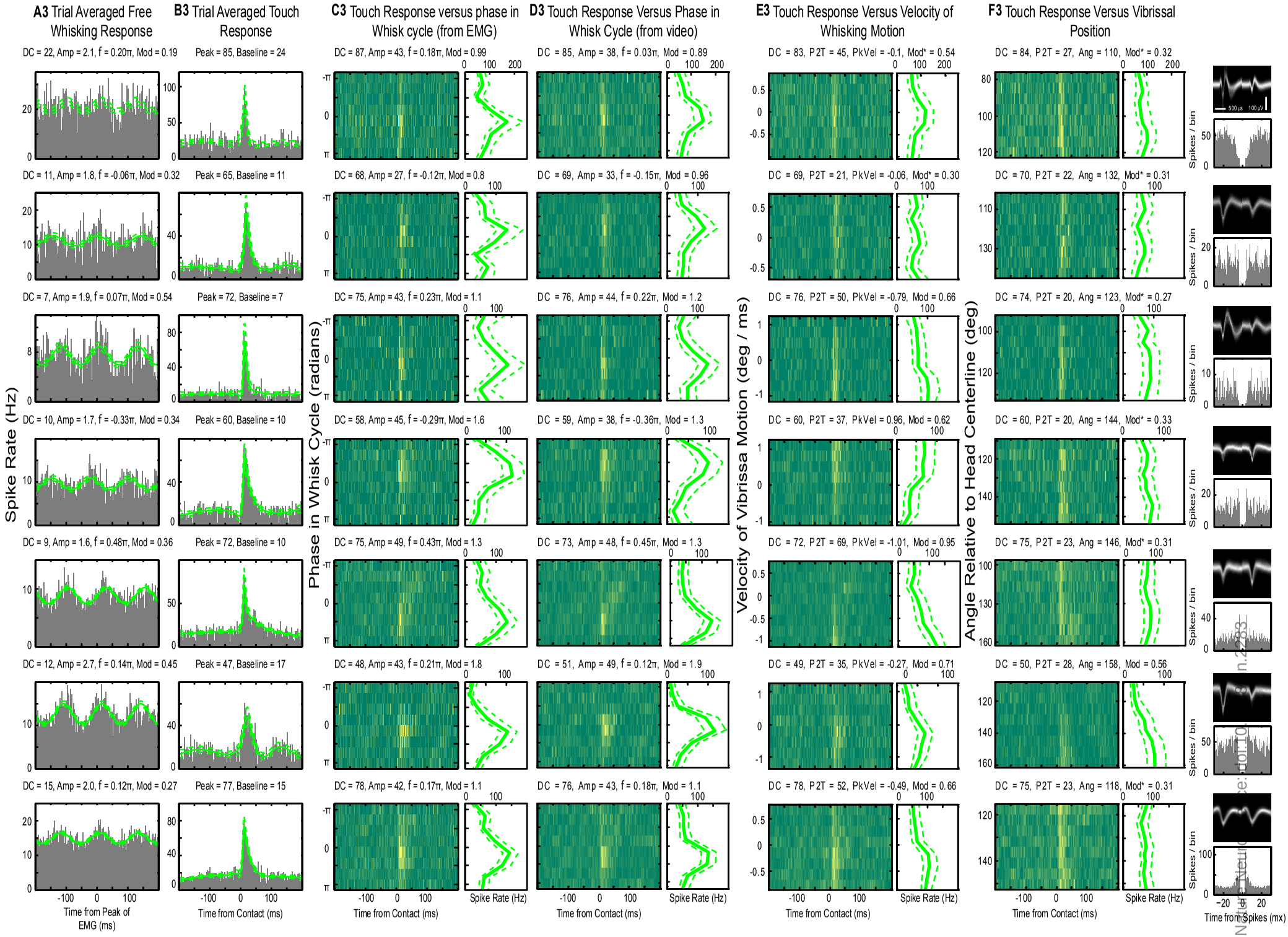

Figure S8 (15-21) - Curtis and Kleinfeld

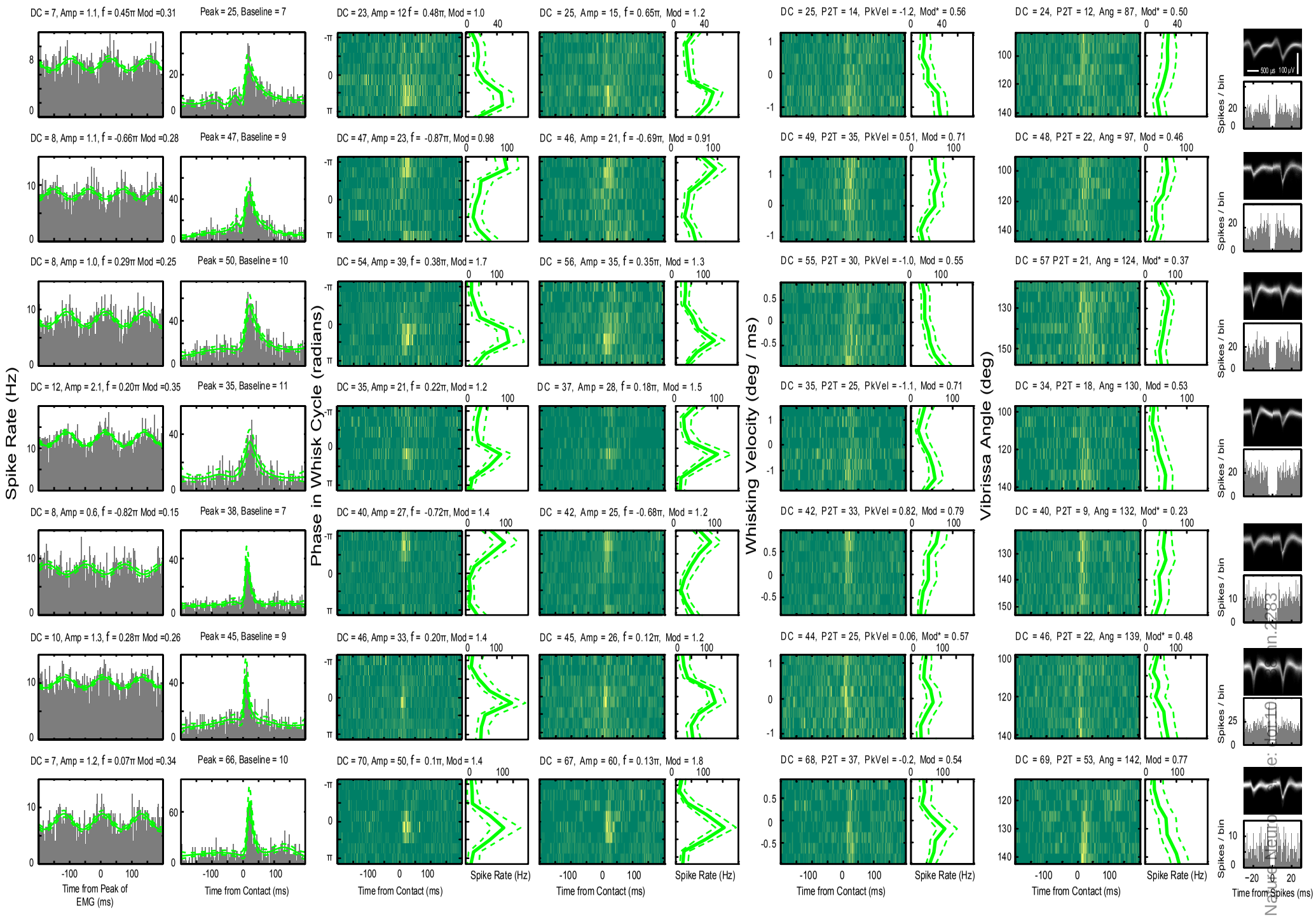

Figure S8 (22-28) - Curtis and Kleinfeld

Figure S9. Free whisking and touch responses for all units with rapid response to touch that are not modulated by phase in the whisk cycle. **(A).** Average spike response histograms in response to free whisking centered on EMG peaks with sinusoid fits (green lines) and resultant parameters defined in caption for figure S8. An asterisk denotes insignificant fit. **(B)** Average spike responses to touch with BARS fits (green lines). Peak and baseline rates calculated from smooth curve are listed above each plot. **(C)** Average touch response histograms parsed by phase in the whisk cycle. **(D)** Plots of the peak values of the touch response from fits to each of the eight intervals of the smooth curve touch responses in panel C. The parameters listed above each plot were estimated by fitting a sinusoid to each curve and have the same designation as in panel A. Dotted lines indicate 95 % confidence intervals for mean spike rate estimates. **(E)** Autocorrelations and waveforms for each neuron.

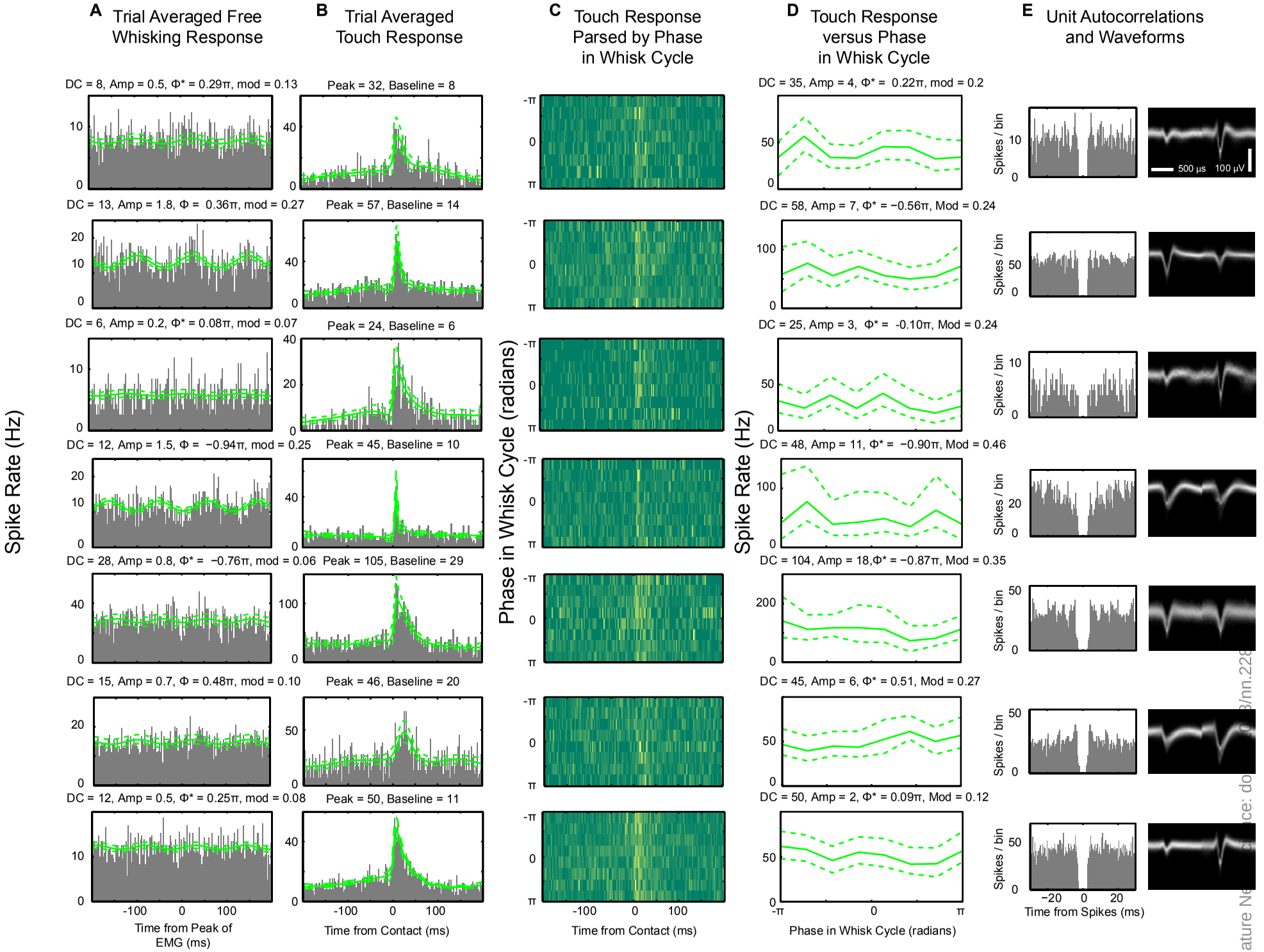

Figure S9 - Curtis and Kleinfeld

Figure S10. Comparisons of maximum touch response and modulation depth at different preferred phases. **(A)** The spike rate for the maximum touch response as a function of preferred phase for units with whisking modulated rapid touch responses. **(B)** The modulation depth of the touch response plotted as a function of each unit's preferred phase. Mean values across all preferred phases are indicated in each plot by dark green line along with 95 % confidence band in light green. There is no significant tendency for either maximum touch response amplitude or modulation depth to be greater at any specific preferred phase relative to other preferred phases.

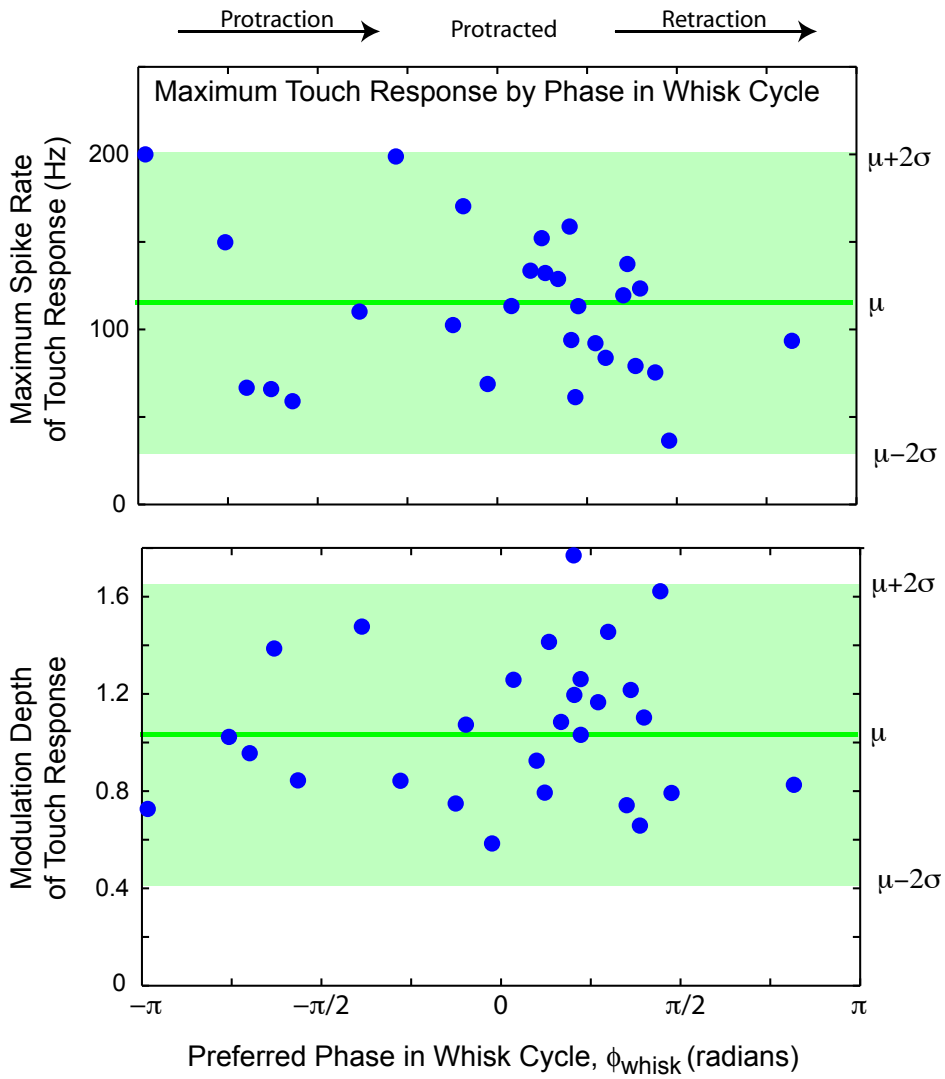

Nature Neuroscience: doi:10.1038/nn.2283

Figure S10 - Curtis and Kleinfeld

Figure S11. The preferred phase in the whisk cycle for contact estimated from ∇EMG data versus videographic data. The slope of the best fit line is 0.92 ($p < 0.001$).

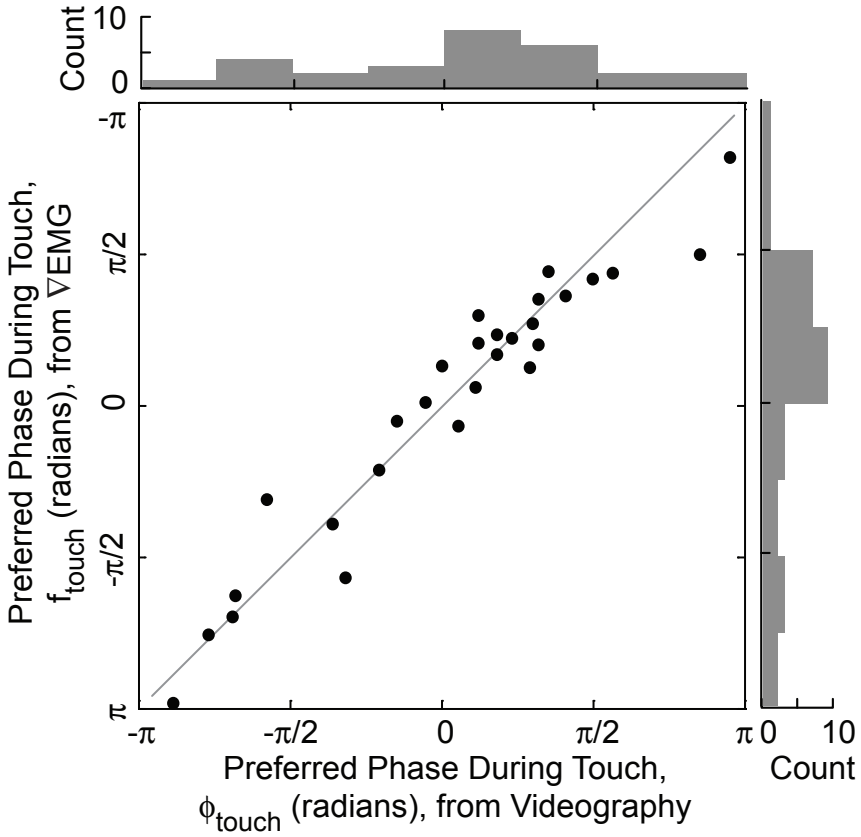

Figure S11 - Curtis and Kleinfeld

Nature Neuroscience: doi:10.1038/nn.2283

Supplemental Material for NN-A26718-T
"Phase-to-rate transformations encode touch in cortical neurons of a scanning sensorimotor system" by John Curtis and David Kleinfeld

Figure S12. Touch responses as a function of phase in the whisk cycle for changes in whisking parameters. Shown are examples, including that for unit 3 shown in figure 6 of the main text.

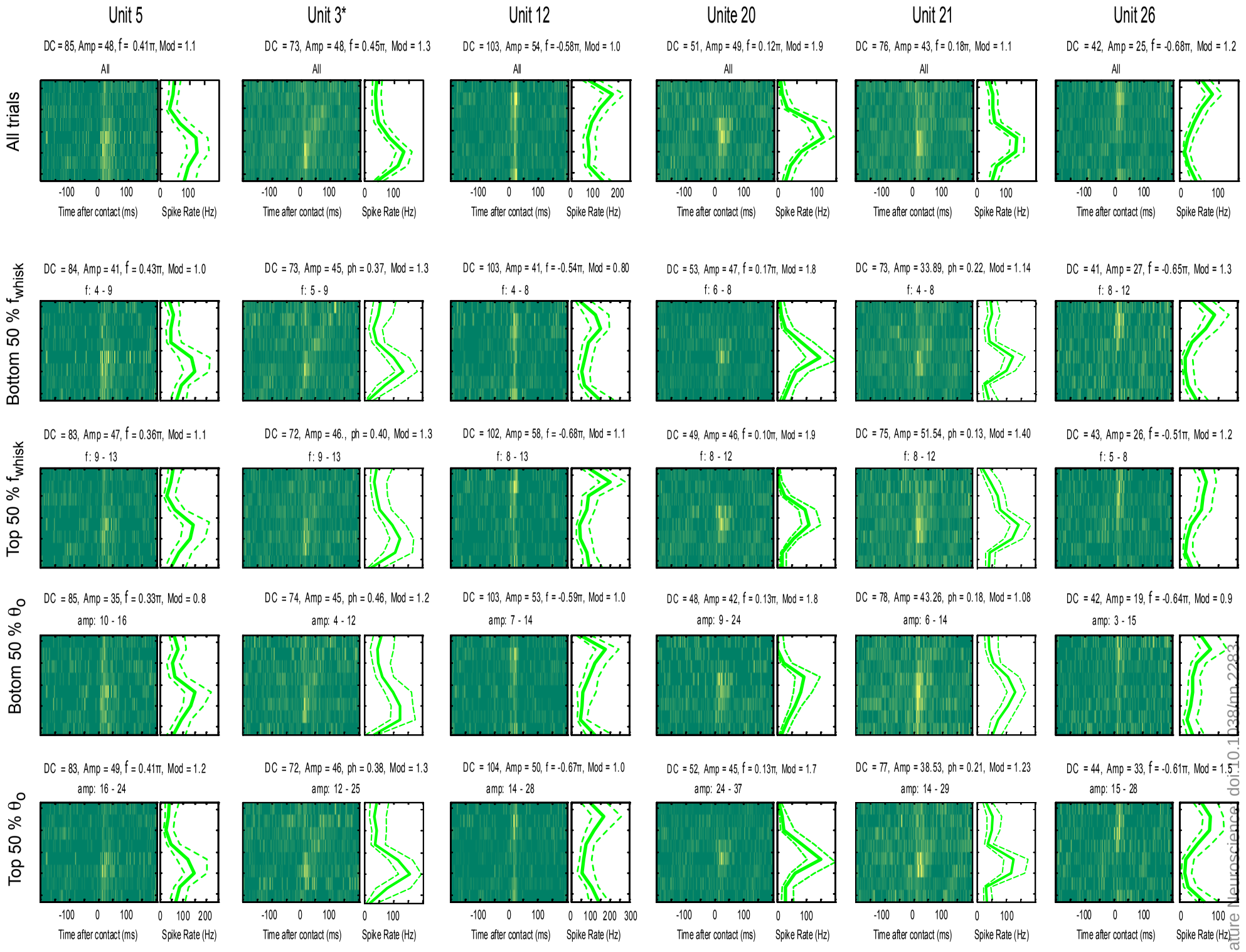

Nature Neuroscience doi:10.1038/nn.2283

Figure S12 - Curtis and Kleinfeld